ISSN : 0974 - 7524 Volume 9 Issue 8

Physical CHEMISTRY
An Indian Journal

Full Paper

PCAIJ, 9(8), 2014 [292-300]

Characterization of hydrophobicities of 6-amino-4-phenyltetrahydroquinoline derivatives as antagonists for FSH-receptor using precise electronic features

Mahmood Sanchooli*, Massoud Nejati Yazdi, Fahimeh Khorrami
Chemistry Department, University of Zabol, Zabol, (IRAN)
E-mail : sanchooli@uoz.ac.ir

ABSTRACT

This work was devoted on quantum mechanical *ab initio* study on hydrophobicity 6-amino-4-phenyltetrahydroquinoline derivatives as antagonist for FSH- receptor. The electronic structures were obtimized based on gerneral interaction properties function. A family descriptors of electrostatic potentials, localized ionization energies and carbon chemical shifts discriptors were computed using the Gaussian98 software. Multiple linear regression was used to achieve a reliable QSPR model to predict the hydrophobicity of 6-amino-4-phenyltetrahydroquinoline derivatives within average absolute errors of 5.0%. The accuracy of developed model was confirmed using different types of internal procedures. It was found that quantum mechanical source of dispersion forces has less contribution on hydrophobicity of 6-amino-4-phenyltetrahydroquinoline derivatives, whereas the charge transfer interactions, surprisingly, show the major impact on their hydrophobicity properties.

KEYWORDS

Hydrophobicity;
FSH- receptor;
Charge transfer;
Lone pairs;
Local ionization energy.

INTRODUCTION

Hydrophobicity is one of the most important physicochemical parameters associated with chemical compounds. It represents the tendency of a substance for repelling water molecules and is a parameter that describes the behavior of a solute into polar and nonpolar phases. Therefore, several studies have been carried out to understand, evaluate and predict this parameter for molecules of interest[1-8]. It is because the major properties of biological molecules such as transportation, distribution, metabolic activity, molecular recognition and protein folding are governed by their hydrophobicities. In order to explore the physical or chemical types of molecular interactions, such as hydrophobing effects for even non-synthesized targeting molecules, QSAR/QSPR methods have found to be of promising theoretical techniques[9]. In which, physicochemical or biological properties of a series of molecules are connected to their molecular structure variables[10,11]. The chemical properties of interest could be boiling and melting points, acid-base behavior, chromatographic retention indices, reaction kinetics and equilibriums, partitioning phenomena, and so on. Basically, QSAR/QSPR stud-

ies strongly depend on the molecular descriptors.

Recently QSAR/QSPR researches are mainly focused on proposing new structurally informative, and highly correlated descriptors toward the dependent features. In this regard, quantum mechanical electronic variables have shown more contribution than the regular classical descriptors[12].

The substituted 6A4PTHQD known as *in vitro* highly effective antagonists for the G_s-protein-coupled human follicle-stimulating hormone (FSH) receptor. They use a CHO cell line in order to testify the human FSH receptor. The analyze on relatively all physiologically relevant rat granulosa cells shows a submicromolar IC_{50} concentration which found to significantly inhibit follicle growth and ovulation in an *ex vivo* mouse model. A new nonsteroidal idea of contraception might be achieved through the recent compounds[13]. In a SAR study done by Manivannan *et al.*, the hydrophobicities of 6A4PTHQD have been shown to have a key role in their biological activities[14]. They have demonstrated that the correlation between Clog*P* and observed FSH-receptor antagonistic activity is excellent in terms of the statistical parameters provided 81.1 percent variance in FSH receptor antagonistic activity among the 19 compounds. Their study has revealed that a hydrophobic interaction, as a dominant intermolecular interaction between these ligands and FSH-receptor, governs their activities as antagonists. Their model enables one to predict the antagonistic activities among all 6A4PTHQD; however, the mechanism of the hydrophobic interactions is not well understood and need more precise electronic studies to be performed. In this article, attempts were done to conduct a QSPR study on hydrophobicity of 19 compounds of 6A4PTHQD. Different categories of electronic descriptors, including electrostatic potentials, local ionization energies and carbon chemical shifts were applied to construct the models. In this regard, quantum descriptors of any individual molecule were calculated. Multiple linear regression (MLR) analysis was employed to explore the relevant electronic descriptors affecting the hydrophobicities of the compounds.

EXPERIMENTAL

All calculations were run on a 2.5 GHz Intel® Core™2 Quad Q 8300 CPU with 2 GB of RAM using all four available cores under Windows XP operating system. Modeling and geometry optimization of all molecular structures (Z-matrix) were employed by HyperChem (version 7.1, HyperCube, Inc.)[15]. For full optimization of molecular structures and calculation of quantum chemical descriptors, Gaussian 98 software was used. Variable selection was performed by using SPSS software version 11.5.0 (SPSS Inc., 2001) by employing the multiple linear regression method.

The values of hydrophobicities of nineteen 6A4PTHQD TABLE 1 were taken from ref.[14]. We draw the molecular structures in HyperChem Software and pre-optimized each molecule using the semiemperical method of AM1 as a prior step[15]. Then, the density functional theory (DFT) B3LYP/6-31G* functional/basis set combination was used as implemented in the Gaussian98 software package to re-optimize the molecular geometries of the compounds to compute their electrostatic potentials V (r) on the molecular surfaces defined by the 0.001 au contour of the electron density $\rho(r)$ [16]. Force constants and frequencies were considered to be sure that the geometry is at the minimum value. The electrostatic potential $V_s(r)$ that is created in space around a molecule by its nuclei and electrons was calculated by applying the following equation:

$$V_s(r) = \sum_A \frac{z_A}{|R_A - r|} - \int \frac{\rho(r')dr'}{|r' - r|} \quad (1)$$

where z_A is the charge on nucleus A, located at R_A. The first term on the right side of Eq. (1) is the nuclear contribution to $V(r)$ which is positive; the second term is due to the contribution of electrons which is, consequently, and accordingly negatives[16,17].

The average local ionization energy, $\bar{I}(r)$, is defined as:

$$\bar{I}(r) = \frac{\sum_i \rho_i(r)|\varepsilon_i|}{\rho(r)} \quad (2)$$

Where $\rho_i(r)$ is the electron density of molecular orbital at the point; ε_i is its orbital energy and $\rho(r)$ is the electronic density function. The $\bar{I}(r)$, is interpreted as the average energy required to remove an electron from a point r in the space of an atom or a molecule[18,

Full Paper

TABLE 1 : The 6A4PTHQD, reported (ref. 14) and predicted hydrophobicities Clog p, values.

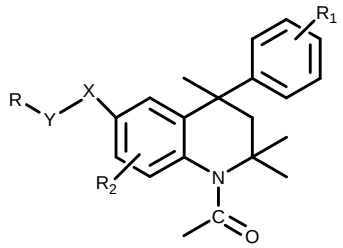

NO.	X	Y	R	R1	R2	Dv.%	ClogP-calc.	ClogP-rept.
1	NH	CO	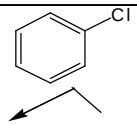	H	6.31	5.96	5.54	5.54
2	NH	CO		H	H	4.8	4.99	-4.08
3	NH	CO	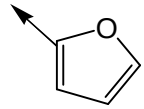	H	H	4.57	4.58	-0.24
4	NH	CO	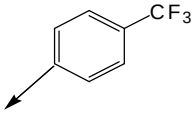	H	H	6.63	6.59	0.61
5	NH	CO	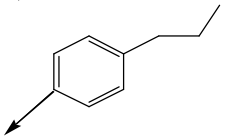	H	H	6.95	6.75	2.83
6	NH	CO	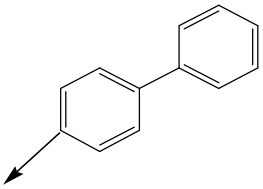	H	H	7.28	7.68	-5.49
7	NH	CO	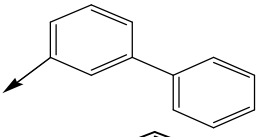	H	H	7.28	7.14	1.96
8	NH	CO	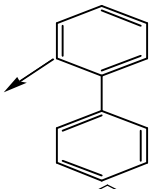	H	H	6.82	7.29	-6.89
9	NH	SO2	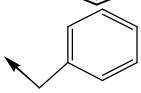	H	H	5.38	5.64	-4.84
10	NH	CONH	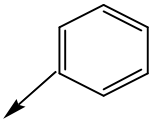	H	H	5.75	6.16	-7.11
11	NH	Bond	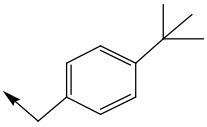	H	H	7.66	7.62	0.47

NO.	X	Y	R	R1	R2	Dv.%	ClogP-calc.	ClogP-rept.
12	CO	NH	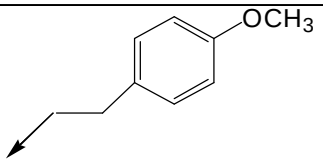	H	H	5.78	5.74	0.65
13	NH	CO	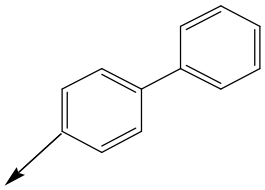	4-Me	H	7.78	7.47	4.03
14	NH	CO	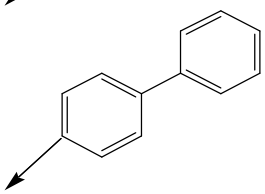	2-OMe	H	7.20	7.02	2.51
15	NH	CO	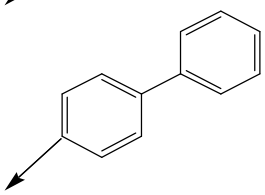	4-OH	H	6.62	6.99	5.57
16	NH	CO	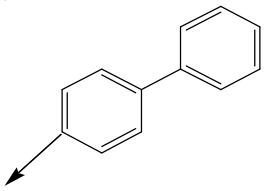	H	7-Me	7.13	7.22	-1.36
17	NH	CO	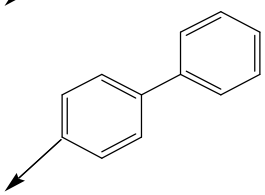	H	8-OMe	7.38	7.71	-4.41
18	O	CO	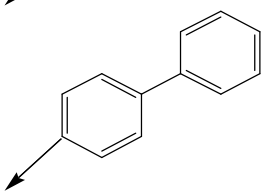	H	H	8.34	8.51	-2.08
19	O	CH2	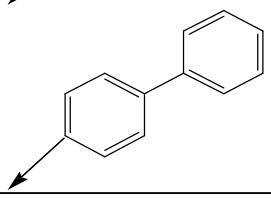	H	H	8.55	8.50	0.53

[19]. $V_s(r)$ is the effective non-covalent interactions, which are largely electrostatic in nature, while $\bar{I}_s(r)$ is more suitable when charge transfer (electron pair donor-electron pair acceptor interaction) occurs. The $V_s(r)$ could also predicts sites for electrophilic and nucleophilic bond forming attack, by means of its most negative and positive regions. However, $V_s(r)$ is not consistently reliable in this respect, because the regions of most negative $V_s(r)$ do not always correspond to the sites where the most reactive electrons are located. For instance, the most negative $V_s(r)$ in benzene derivatives such as aniline, phenol, fluoro- and chlorobenzene, and nitroben-

Full Paper

zene are associated with the substituents; whereas electrophilic reaction occurs on the rings. In contrast, $\bar{I}_s(r)$ correctly predicts the *ortho/para*- or *meta*-directing effects of the substitutes as well as the activation or deactivation of the ring[18].

Politzer et al. demonstrated that the general interaction properties function (GIPF) can be summarized as the following equation[17,20]:

$$\begin{aligned}&\textbf{Property} = f(\nu_{mv}, A_s^{tot}, A_s^{+}, A_s^{-}, V_{s,max}, V_{s,min}, \\ &\bar{V}_s, \bar{V}_s^{+}, \bar{V}_s^{-}, \pi^{tot}, \delta^{tot}, \delta_{+}^{2}, \delta_{-}^{2}, \nu, \bar{I}_{s,max}, \bar{I}_{s,min}, \bar{I}_{s,} \\ &\delta_{\bar{I}S}^{2}, \pi_{\bar{I}S})\end{aligned} \quad (3)$$

We used the WFA statistical analysis program to compute most of GIPF descriptors using the produced CUBE file with Gaussian98 software package[18]. In Eq. (3), ν_{mv} is the molecular volume; $A_s^{tot}, A_s^{+}, A_s^{-}$ are total surface area and the surface area over which $V_s(r)$ is positive and negative, respectively. Politzer et al. showed that the molecular volume is related to the polarizability of the molecule, then they used this descriptor in GIPF approach[21,22]. The $V_{s,\max}, V_{s,\min}$, respectively, are the maximum and minimum values of the electrostatic potential on the molecular surface; $\bar{V}_s, \bar{V}_s^{+}$ and $\bar{V}_s^{-}$, in turn, are the average potentials and averages of positive and negative potentials computed as:

$$\bar{V}_s = \frac{1}{t}\sum_{i=1}^{t} V_s(r_i),\ \bar{V}_s^{+} = \frac{1}{m}\sum_{j=1}^{m} \bar{V}_s^{+}(r_j),\ \bar{V}_s^{-} = \frac{1}{n}\sum_{k=1}^{n} \bar{V}_s^{-}(r_k) \quad (4)$$

The π^{tot} is the average deviation of overall potentials computed as:

$$\pi = \frac{1}{t}\sum_{i=1}^{t} \left| V_s(r_i) - \bar{V}_s \right| \quad (5)$$

The π interpreted as an indicator of internal charge separation, which is presented even in molecules having zero dipole moment due to symmetry, e.g. *para*-dinitrobenzene and boron trifluoride. The δ_{tot}^2, δ_{+}^2 and δ_{-}^2 are total positive and negative variances of electrostatic potentials, respectively, calculated as follows:

$$\delta_{tot}^2 = \delta_{+}^2 + \delta_{-}^2 = \frac{1}{m}\sum_{j=1}^{m}\left[V_s^{+}(r_j) - \bar{V}_s^{+}\right]^2 + \frac{1}{n}\sum_{k=1}^{n}\left[V_s^{-}(r_k) - \bar{V}_s^{-}\right]^2 \quad (6)$$

where ν is the electrostatic balance parameter computed as[21]:

$$\nu = \frac{\delta_{+}^2 \delta_{-}^2}{\left[\delta_{+}^2 + \delta_{-}^2\right]} \quad (7)$$

In these summations, t is the total number of points on the surface grid; m and n are the numbers of points when $V(r)$ is positive and negative, respectively[18]. The features of $\bar{I}(r)$ could be characterized analogously to those of , its extrema , $\bar{I}_{s,\max}$, $\bar{I}_{s,\min}$, its average magnitude $\bar{I}_s$, average deviation ($\pi_{\bar{I}_S}$), and variance ($\delta_{\bar{I}_S}^2$) keeping in mind that $\bar{I}(r)$ only has positive values[17,18,23,24]. In order to have better verification on the effects of non-covalent interactions, we calculated polarizability (α) and carbon chemical shifts (δ_C) in separate Gaussian jobs, using HF/3-21G freq and HF/3-21G nmr=giao keywords, respectively. The latter descriptor can be obtained as:

$$\delta_C = \mathrm{ICS}_{\mathrm{reference}} - \mathrm{ICS} \quad (8)$$

where $\mathrm{ICS}_{\mathrm{reference}}$ and ICS, refer to the isotropic chemical shielding of tetra methyl silan as reference and the isotropic chemical shielding of any carbon on the parent molecule Figure 1.

In TABLE 2, a list of all quantum descriptors that were obtained using *ab initio* calculation are introduced. Their corresponding values are provided in the supporting information.

RESULTS AND DISCUSSION

The chemical structures of nineteen 6A4PTHQD TABLE 1 were optimized and their corresponding electronic along with their carbon NMR chemical shift descriptors were calculated. The most important variables are selected by a stepwise selection procedure, which combines the forward selection and backward elimination approaches. This procedure, firstly, considered the

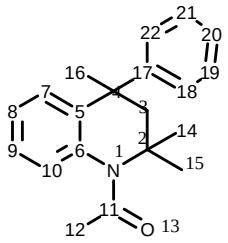

Figure 1 : The relative position of carbon atoms in the parent molecule of 6A4PTHQ which are subjected in carbon chemical shift calculations.

descriptive variable which is most highly correlated with the response. If the inclusion of this variable results in a significant improvement of the regression model, evaluated with an overall *F*-test, it is retained and the selection continues. In the next step, the variable that gives the largest significant decrease of the regression sum of squares, evaluated with a partial F-test, is added. After each forward selection step, a backward elimination step is performed. In this step, a partial *F*-test for the variables, already in the equation, is carried out. If a variable does not significantly contribute to the regression model, it is removed. The procedure terminated at the moment that no variable fulfills the requirements anymore. After this, the classical MLR can be applied to the retained variables to build a predictive model.

The stepwise variable selection-based MLR analysis was employed to obtain the structure-property relationships between reported hydrophobicities and electronic descriptors of nineteen 6A4PTHQD.

$$\begin{aligned} \mathrm{CLog(p)} &= 15.11(\pm 3.03) + 0.022\ \alpha(\pm 0.003) \\ &- 0.029\ V_{s,max}(\pm 0.007) - 0.037\ C_5(\pm 0.01) \\ &+ 1.127\ \delta^2_{\bar{I}_S}(\pm 0.212) - 0.554\ \bar{I}_{s,max}(\pm 0.131) \\ &N = 19,\ R^2 = 0.947,\ SE = 0.29,\ F = 46.18, \\ &Q^2_{LOO} = 0.872,\ Q^2_{LMO} = 0.805 \end{aligned} \quad \textbf{(9)}$$

The values in the parenthesis represent the standard deviation of the coefficients. The symbols N, R^2, SE and F are the numbers of components, correlation coefficients, standard error of regression and Fisher's F-ratios, respectively. The correlation coefficients of leave-one-out and leave-many-out cross-validations are denoted by Q^2_{LOO} and Q^2_{LMO}, respectively.The R^2 value of 0.947 describes that the resultant equation can

TABLE 2 : Brief description of calculated quantum chemical descriptors

Quantum descriptor	Definition
$V_{s,\min}$	The maxima of electrostatic potential on the molecular surface
$V_{s,\min}$	The minima of electrostatic potential on the molecular surface
$\overline{V}_s^+$	Average of positive potentials
$\overline{V}_s^-$	Average negative potentials
π^{tot}	The average deviation of overall potentials
δ^2_{tot}	Total variances of electrostatic potentials
δ^2_+	Positive variances of electrostatic potentials
δ^2_-	Negative variances of electrostatic potentials
ν	Electrostatic balance parameter
$\bar{I}_s(r)$	Average local ionization energy to remove an electron
$\bar{I}_{s,\max}$	The maxima of average local ionization energy
$\bar{I}_{s,\min}$	The minima of average local ionization energy
$\pi_{\bar{I}_S}$	Average deviation of average local ionization energy
$\delta^2_{\bar{I}_S}$	The variance of average local ionization energy
α	Polarizability of molecule
δ_C	Carbon chemical shift

Full Paper

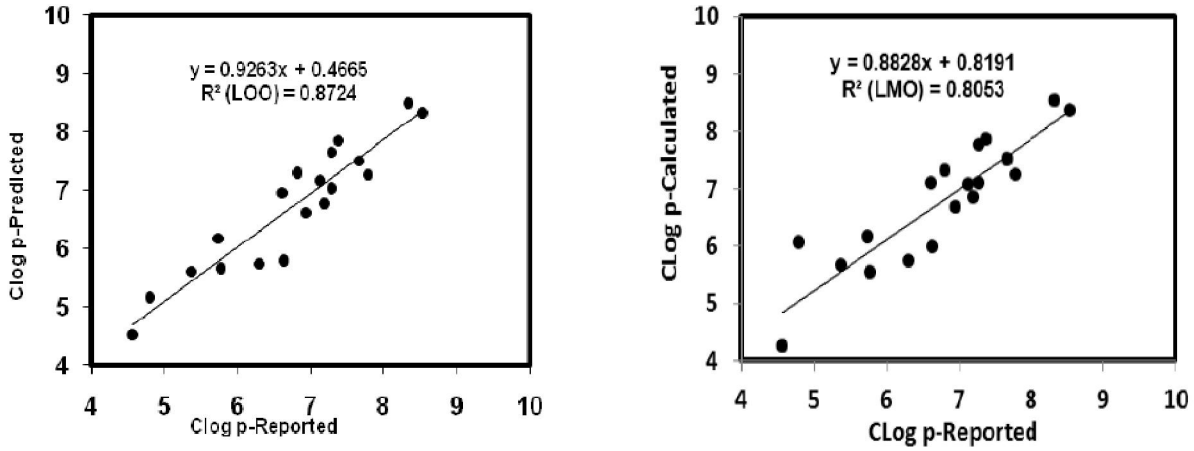

Figure 2 : Plot of leave-one-out and leave-many-out cross-validation hydrophobicity of 6A4PTHQD.

explain about 94.7 percent of variance in the CLog(p) data of the 6A4PTHQD where as the high value of cross-validated coefficients $Q_{LOO} = 0.872$, $Q_{LMO} = 0.805$ as well as their closeness to each other explain the predictive power and stability of the proposed model Figure 2.

The widely used approach to establish the robustness of the resulting models is called Y-randomization. The values of CLog(p) were randomly attributed to the molecules and the MLR modeling was repeated with the randomized data. The randomization was repeated one hundred times and the maximum values obtained for the R^2 and RMS were 0.56 and 0.29, respectively. The statistical qualities of these models are much lower than the original one. Therefore, it can be considered that the model is reasonable and had not been obtained by chance.

This model was used to reproduce the hydrophobicity of 6A4PTHQD. Results are shown in TABLE 1.

In order to inspect the relative importance and contribution of each descriptors in the constructed model, the value of mean effect (MF) was calculated for each descriptor by the following equation and is shown in Figure 3.

$$\mathbf{MF_j} = \frac{\beta_j \sum_{i=1}^{n} d_{ij}}{\sum_{j=1}^{m} \beta_j \sum_{i=1}^{m} \sum_{i=1}^{n} d_{ij}} \quad \textbf{(10)}$$

where MF_j is the mean effect of considering descriptor; j and β_j, respectively, are the coefficients of descriptors j and d_{ij} denotes the value of descriptor j of molecule I; m is the number of descriptors in the model and n is the number of molecules in the data sets. The value of mean effect shows the relative contribution of each descriptor on the predicted response.

The penta-parametric Eq.(9) indicates that dispersive forces, dipolar and charge transfers interactions govern the hydrophobicity property of 6A4PTHQD in a solution. Maximum electrostatic potential $V_{s,max}$ which is the highest positive site on box of molecule and stands for non-covalent interactions, along with polarizability α, are the measure of quantum mechanical london dispersive forces. We believe that the carbon chemical shifts might be due to the polar bonds in 6A4PTHQD molecules. The charge transfer contribution in hydrophobicity of 6A4PTHQD is clearly reflected in variance value and maximum value of local ionization energy descriptors of $\delta^2_{\bar{I}_s}$ and $\bar{I}_{s,max}$, respectively.

Concerning the model Eq. (9), polarizability α and the maximum positive potential site $V_{s,max}$ have positive and negative coefficients, respectively. While the polarizability increases the hydrophobicity property, the high positive potential site, shows a negative impact on hydrophobicity indicating the potentially electrophilic attacking site on the 6A4PTHQD. Moreover, the model proposes carbon 5 as the reactive carbon with negative impact on hydrophobicity close to amide linkage, X – Y = NH – (CO) Figure 1. This might be expected as carbon 5 is deshielded by inducing ring magnetic field effect of penile group situated on carbon 4 which consequently decreases the hydrophobicity. Among the three different types of interactions, local ionization energy shows the highest impact on hydrophobicity as model Eq. (9) concerns Figure 3. The negative sign of

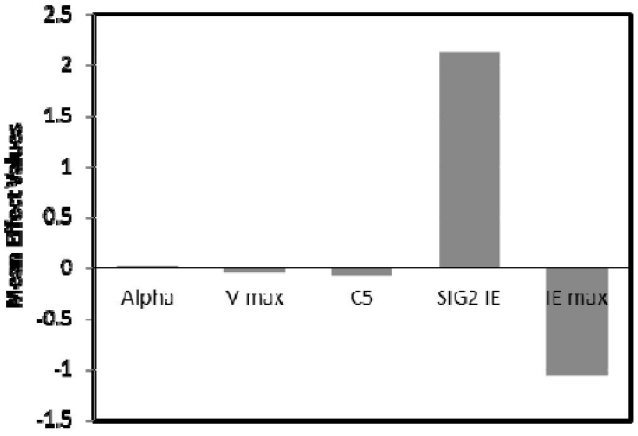

Figure 3 : The mean effect values of contributed descriptors in hydrophobicity of 6A4PTHQD. $(Alpha = \alpha, V\ max = V_{max}, C5 = \delta_{C5}, SIG2\ IE = \delta_f, IE\ max = I_{s,max})$

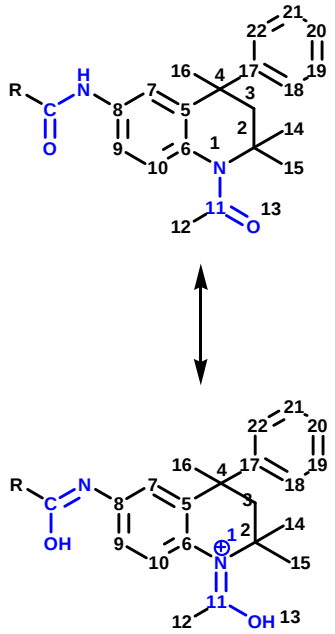

Figure 4 : A proposed model for intra-molecular charge (proton) transfer in 6A4PTHQD.

the maximum value of local ionization energy in hydrophobicity equation seems normal as it indicates that charge transfer between 6A4PTHQD is mostly due to inter molecular hydrogen bondings. However, the positive sign of variance of localized ionization energy in Eq. (9) is unexpected which is probably could be explained by the intra-molecular charge transfers of keto-enol tautomerism. This tautomerism increases the hydrophobicity because the lone pairs and proton of 6A4PTHQD are more involved inside the solute Figure 4. In the other word, there exists a competition between inter- and intra-molecular charge transfers for 6A4PTHQD controlling their hydrophobicity. While the former show decreasing effect, the latter has an increasing contribution, as model concerns.

CONCLUSION

The structures of a series of nineteen derivatives of 6A4PTHQ as antagonists for the Gs-protein-coupled human follicle-stimulating hormone (FSH) receptor were optimized, using quantum mechanical *ab intio* calculation. Electrostatic potential, localized ionization energy and carbon shift NMR descriptors with a total matrix of sixteen variables was obtained. Using multiple linear regression method, a reliable model was established to predict the hydrophobicity of 6A4PTHQD within an average absolute error of 5.0%. Results proposed that london dispersion forces had less contribution on hydrophobicity of these derivatives, whereas the charge transfer interactions, surprisingly, showed the major impact on their hydrophobicities.

ACKNOWLEDGMENTS

The authors thank to the Research Council of Zabol University for financial support of this project. We are also indebted to thank Alireza Samzadeh for his constructive discussions and recommendation.

REFERENCES

[1] E.Benfenati, G.Gini, N.Piclin, A.Ronaglioni, M.R.Vari; Chemosphere, **53**, 1155-1164 **(2003)**.
[2] P.A.Carrupt, B.Testa, P.Gaillard; Rev.Computational Chem., Wiley-VCH, **11**, 241-315 **(1997)**.
[3] X.Q.Kong, D.Shea, W.A.Gebreyes, X.R.Xia; Anal.Chem., **77**, 1275-1281 **(2005)**.
[4] A.J.Leo, P.Y.C.Jow, C.Silipo, C.Hansch; J.Med.Chem., **18**, 865-868 **(1975)**.
[5] T.Masuda, T.Jikihara, K.Nakamura, A.Kimura, T.Takagi, H.Fujiwara; J.Pharm.Sci., **86**, 57-63 **(1997)**.
[6] D.E.Smith, A.D.J.Haymet; Rev.Computational Chem.Wiley-VCH, **19**, 43 **(2003)**.
[7] M.Totrov; J.Comput.Chem., **25**, 609-619 **(2004)**.
[8] L.Xing, R.C.Glen; J.Chem.Inf.Comput.Sci., **42**,

796-805 **(2002)**.

[9] C.Hansch, T.Fujita; J.Am.Chem.Soc., **86**, 1616-1626 **(1964)**.

[10] A.R.Katritzky, A.Lomaka, R.Peturkhin, R.Jain, M.Karelson, A.E.Visser, R.D.Rogers; J.Chem.Inf.Comput.Sci., **42**, 71-74 **(2002)**.

[11] M.Staikova, P.Messih, Y.D.Lei, F.Wania, D.J.Donalson; J.Chem.Eng.Data, **50**, 438-443 **(2005)**.

[12] J.Wang, L.Zhang, G.Yang, C.G.Zhan; J.Chem.Inf.Comput.Sci., **44**, 2099-2105 **(2004)**.

[13] N.C.R.Van Straten, T.H.J.Van Berkel, D.R.Demont, W.J.F Karstens., R.Merkx, J.Oosterom, J.Schulz, R.G.van Someren, C.M.Timmers, P.M.Van Zandvoort; J.Med.Chem., **48**, 1697-1700 **(2005)**.

[14] E.Manivannan, S.Prasanna; Bioorganic & Medicinal Chemistry Letters, **15**, 4496-4501 **(2005)**.

[15] HyperChem Release 7.1 for Windows Molecular Modeling System Program 660 Package, HyperCube, **(2002)**.

[16] J.S.Murray, P.Politzer, M.C.Concha; J.Mol.Model., **13**, 643-650 **(2007)**.

[17] P.Politzer, J.S.Murray, F.A.Bulat; J.Mol.Model., **16**, 1731-1742 **(2010)**.

[18] F.A.Bulat, A.Toro-Labbe, T.Brinck, J.S.Murray, P.Politzer; J.Mol.Model., **16**, 1679-1691 **(2010)**.

[19] P.Kulshrestha, N.Sukumar, J.S.Murray, R.F.Giese, T.D.Wood; J.Phys.Chem.A, **113**, 756-766 **(2009)**.

[20] P.Politzer, J.S.Murray; Fluid Phase Equilibria, **185**, 129-137 **(2001)**.

[21] P.Jin, J.S.Murray, P.Politzer; Int.J.Quantum Chem., **96**, 394-401 **(2004)**.

[22] O.G.Gonzalez, J.S.Murray, Z.Peralta-Inga, P.Politzer; Int.J.Quantum Chem., **83**, 115-121 **(2001)**.

[23] P.Politzer, J.S.Murray, F.Abu-Awwad; Int.J.Quantum Chem., **76**, 643-47 **(2000)**.

[24] P.J.T.Brinck, J.S.Murray, P.Politzer; Int.J.Quantum, Chem., **95**, 632-637 **(2003)**.